Ring Expansion in Methylene Pyrrole Radicals. Quantum Chemical Calculations

Faina Dubnikova and Assa Lifshitz*

Department of Physical Chemistry, The Hebrew University of Jerusalem, Jerusalem 91904, Israel

Received: June 24, 1999; In Final Form: September 9, 1999

Ring expansions in *N*-methylene pyrrole, 2-methylene pyrrole, and 3-methylene pyrrole radicals were studied by the Becke three-parameter hybrid method with Lee−Yang−Parr correlation functional approximation (B3LYP). Structure, energy, and frequency calculations were carried out with the Dunning correlation consistent polarized double ξ (cc-pVDZ) and augmented aug-cc-pVDZ basis sets. The potential energy surfaces for ring expansion in methylene pyrrole contain several intermediates and transition states. The process, which takes place by insertion of the methylene group into the pyrrole ring in the three isomers, occurs via two principal mechanisms. One mechanism is associated with cleavage of the C−N or C−C bonds of the pyrrole ring already in the first step. In the second mechanism, the transition states of the first stage consist of a new three-membered ring and the original pyrrole ring fused together. In all the three isomers of methylene pyrrole, the reaction pathways leading to ring expansion include intermediates that, via additional transition states, lead to the production of hydropyridyl radical. The latter, by a very fast H-atom ejection, produces pyridine. Ring expansion in the molecule *N*-methylpyrrole does take place, but the energy level of the transition state is very high. The reaction coordinate in the process is cleavage of the C−N bond and a C−H bond of the methyl group, which from a kinetic viewpoint is equivalent to ejection of a H atom from the molecule and ring expansion in *N*-methylene pyrrole. The structure and energetics of the various pathways are shown.

I. Introduction

Expansion of five- to six-membered rings is an important process in combustion chemistry. The interconversion of the benzene and cyclopentadiene rings plays an important role in many combustion processes.[1,2] Such an interconversion takes place also in methylpyrrole, which is a nitrogen analogue of methylcyclopentadiene.[3] It has been found experimentally that one of the major constituents of post-shock mixtures of heated *N*-methylpyrrole is pyridine. It was also found that the addition of toluene as a free radical scavenger suppressed the formation of pyridine, indicating that the formation of pyridine is associated with free radical reactions.[3] It has thus been assumed that ring expansion of the *N*-methylpyrrole skeleton takes place from the *N*-methylene pyrrole radical (following a H-atom ejection from the methyl group in *N*-methylpyrrole), rather then from *N*-methylpyrrole itself.

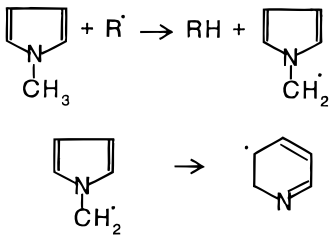

Based on this assumption, a kinetic scheme was constructed, computer modeling was carried out, and a very good agreement between the experiment and the calculation was obtained. Whereas this agreement provided a proof for the free radical route of ring expansion, the rate constant of the process was not measured directly, but rather was obtained by a best fit to the experimental results.

There is a large volume of information on quantum chemical calculations of free radicals.[4−15] Jursic has shown that the structure and energetics of many free radicals, including heterocyclic compounds that contain electronegative atoms such as N, O, S and F, were successfully reproduced by hybrid density functional theory (DFT) methods.[10−15] The Becke three-parameter hybrid method[16] with Lee−Yang−Parr correlation functional approximation[17] (B3LYP) was one of the best methods in the majority of the cases. Moreover, this method also has been successfully used to evaluate activation energies and enthalpy changes in radical reactions.[10−12] Jursic and others have also shown that in almost all the cases, hybrid and nonlocal (BLYP for example) DFT methods outperformed both HF and MP2 ab initio calculations and gave good agreement with measured values.[10] In some cases these methods produced even better results than quadratic CI, including single and double substitutions with a triples contribution to the energy QCISD-(T). Similar agreement between QCISD and B3LYP was observed by Wiberg and co-workers when the computational study of heterosubstituted allyl radicals was performed.[4] We have thus used in this study the B3LYP method with the augmented Dunning correlation consistent polarized valence double ξ (aug-cc-pVDZ) basis set.[18,19]

We are not aware of any quantum chemical calculation on ring expansion processes in *N*-methylpyrrole, neither from the molecule itself nor from a radical, which is obtained by H-atom ejection from the methyl group in the molecule. We are aware, however, of quantum chemical calculations of methyl group migration from the nitrogen to position 2 in the ring.[20] This process has activation energy of some 60 kcal/mol, which is comparable with the barrier found experimentally.

The purpose of this investigation is to provide additional support (or rebuttal) to the assumption concerning the radical character of the ring expansion process. We are also interested

* Author to whom all correspondence should be addressed.

10.1021/jp992113e CCC: $19.00
Published on Web 12/28/1999

TABLE 1: Selected Structural Parameters of the Reactant, Transition States, Intermediate, and Product of *N*-Methylene Pyrrole Ring Expansion, Calculated at uB3LYP/aug-cc-pVDZ Level of Theory

parameter[a,b]	*N*-methylene pyrrole	TS1	INT1	TS2	orthohydro-pyridyl
r-N(1)−C(2)	1.391	1.429	1.491	1.943	2.529
r-C(2)−C(3)	1.377	1.402	1.479	1.410	1.369
r-C(3)−C(4)	1.433	1.429	1.397	1.419	1.416
r-C(4)−C(5)	1.377	1.374	1.394	1.383	1.430
r-N(1)−C(5)	1.391	1.411	1.422	1.387	1.304
r-N(1)−C(6)	1.375	1.458	1.492	1.443	1.456
r-C(6)−C(2)	2.462	1.899	1.511	1.495	1.496
∠C(6)N(1)C(2)	125.78	82.26	60.89	49.66	31.64
∠N(1)C(6)C(2)	27.27	48.22	59.52	82.80	117.71

[a] Distances in Angstroms; angles in degrees. [b] The atom numbering is shown in Figures 1 and 2.

in examining possible ring expansion in other isomers of methylpyrrole, namely 2- and 3-methylpyrrole.

II. Computational Details

Optimization of the ground-state geometry of the radical species was carried out using the Berny geometry optimization algorithm.[21] For determining transition-state structures, we used the combined synchronous transit and quasi-Newton (STQN) method.[22] All the calculations were performed without symmetry restrictions. As a first trial for localizing the various isomers of methylene pyrrole and hydropyridyl, and those of the intermediates and transition states, the B3LYP/cc-pVDZ level of the theory was used. Vibrational frequencies were calculated at the same theoretical level of theory to characterize the optimized structure as a minimum or a first-order saddle point on the potential energy surface. The obtained geometry and the second derivatives were further optimized using the augmented basis set (aug-cc-pVDZ) by the addition of diffuse functions on the all heavy atoms and the hydrogen. To check whether the transition state led to the correct reactant and product, intrinsic reaction coordinate (IRC) calculations with mass-weighted internal coordinates were performed using the cc-pVDZ basis set.

All the calculated frequencies, as well as the zero-point energies, are of harmonic oscillators. Zero-point energies were scaled by the ZPE scaling factor of 0.9806 and the entropies were scaled by the entropy scaling factor of 1.0015.[23] Entropies were calculated using two basis sets, uB3LYP/cc-pVDZ and uB3LYP/aug-cc-pVDZ level, for comparison. The entropies calculated with the aug-cc-pVDZ basis set were used to evaluate preexponential factors of the reactions under consideration.

We have examined the spin contamination before and after annihilation of the radical species. Before annihilation, the $\langle S^2 \rangle$ ranged from 0.755 to 0.787, and after annihilation the value was 0.750. This suggests that the wave functions are not strongly contaminated by states of higher multiplicity.

All the calculations were performed using the GAUSSIAN-94 program package[24] on a DEC Alpha TurboLaser 8200 5/300 at the Institute of Chemistry of The Hebrew University of Jerusalem.

III. Results

Tables 1−3 contain selected parameters of the optimized geometries of the three isomers of methylene pyrrole which are considered to be reactants in this investigation, and two isomers of hydropyridyl as products. As products we refer to the isomers, which are direct precursors of pyridine (i.e., which produce pyridine by a direct ejection of an H atom).

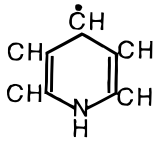

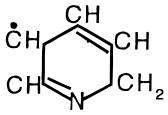

Isomers such as

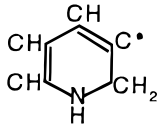

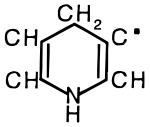

which cannot produce pyridine in one step as they require, for example, 1,2-H-atom migrations but participate in overall potential surface, appear here as intermediates.

Tables 1−3 also contain structures of transition states and intermediates involved in the radical reactions. (See Figure 1 for atom numbering in the tables.) All the structural parameters, which are shown in the tables, were computed at the uB3LYP/aug-cc-pVDZ level of theory. Total energies, scaled zero-point energies, entropies, and relative energies with ZPE corrections are listed in Tables 4−6 calculated at the uB3LYP level of theory for both cc-pVDZ and aug-cc-pVDZ basis sets. The potential energy surfaces of the ring expansion processes of the three isomers of methylene pyrrole are shown in Figures 2−4.

IV. Structures of Critical Points and Energetics Along the Ring Expansion Pathways

***N*-Methylene Pyrrole.** The reaction pathway leading from *N*-methylene pyrrole to one of the hydropyridyl isomers contains two transition states, TS1 and TS2, and one intermediate, INTl. The species involved in this reaction pathway are shown in Figure 2. The figure also shows the location of the high electron density in each species. The main structural parameters along the reaction pathway are shown in Table 1. The changes in the

TABLE 2: Selected Structural Parameters of the Reactant, Transition States, Intermediates, and Product of 2-Methylene Pyrrole Ring Expansion, Calculated at uB3LYP/aug-cc-pVDZ Level of Theory

parameter[a,b]	2-methylene pyrrole	TS3	INT2	TS4	TS5	INT3	TS6	*N*-hydropyridyl
r-N(1)−C(2)	1.396	2.160	3.020	2.881	2.717	2.412	2.493	2.395
r-C(2)−C(3)	1.424	1.369	1.343	1.379	1.361	1.335	1.434	1.425
r-C(3)−C(4)	1.408	1.404	1.422	1.404	1.428	1.469	1.421	1.425
r-C(4)−C(5)	1.393	1.419	1.433	1.435	1.411	1.361	1.376	1.369
r-N(1)−C(5)	1.373	1.307	1.300	1.301	1.324	1.378	1.386	1.400
r-C(2)−C(6)	1.391	1.326	1.305	1.324	1.375	1.496	1.417	1.369
r-N(1)−C(6)	2.462	2.956	3.636	3.210	1.989	1.469	1.418	1.400
∠C(6)C(2)C(3)	130.62	154.09	175.17	161.09	131.06	124.37	114.51	121.13

[a] Distances in Angstroms; angles in degrees. [b] The atom numbering is shown in Figures 1 and 3.

TABLE 3: Selected Structural Parameters of the Reactant, Transition States, Intermediate, and Product of 3-Methylene Pyrrole Ring Expansion, Calculated at uB3LYP/aug-cc-pVDZ Level of Theory

parameter[a,b]	3-methylene pyrrole	TS7	INT4	TS8	TS9	INT5	TSIO	INT6	TS11	*N*-hydropyridyl
r-N(1)−C(2)	1.372	1.389	1.393	1.402	1.362	1.359	1.368	1.380	1.413	1.400
r-C(2)−C(3)	1.412	1.326	1.322	1.344	1.397	1.410	1.398	1.395	1.389	1.369
r-C(3)−C(4)	1.451	2.559	2.807	2.928	1.479	1.560	1.787	2.595	2.532	2.436
r-C(4)−C(5)	1.373	1.328	1.327	1.329	1.428	1.453	1.414	1.350	1.359	1.369
r-N(1)−C(5)	1.383	1.387	1.387	1.387	1.388	1.372	1.368	1.388	1.377	1.400
r-C(3)−C(6)	1.409	1.324	1.316	1.438	1.479	1.491	1.476	1.509	1.438	1.425
r-C(4)−C(6)	2.564	3.231	3.419	3.203	1.789	1.558	1.526	1.504	1.471	1.425
∠C(2)C(3)C(6)	127.03	166.22	171.91	163.73	125.28	120.96	120.78	113.80	116.31	121.13
∠C(2)N(1)C(5)	110.03	120.09	123.68	125.55	111.46	112.71	113.56	122.51	120.83	120.55

[a] Distances in Angstroms; angles in degrees. [b] The atom numbering is shown in Figures 1 and 3.

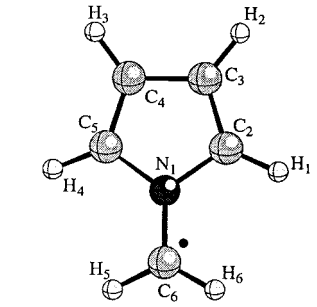

N-methylene pyrrole

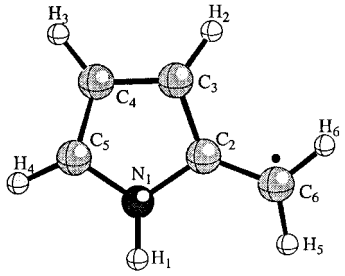

2-methylene pyrrole

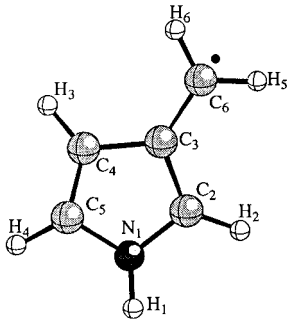

3-methylene pyrrole

Figure 1. Structures of *N*-methylene pyrrole, 2-methylene pyrrole, and 3-methylene pyrrole.

parameters from the reactant to the final product can be viewed by going from left to right. The first stage of the reaction is associated with the methylene group shift from the N atom of the pyrrole ring toward the neighboring carbon atom C(2) via transition state TS1. The reaction coordinate of the transition state is a C(6)N(1)C(2) angle bend that brings C(6) closer to C(2), together with a rotation of the methylene group C(6)-H(5)H(6) with respect to the ring plane (Figure 2). The result is the formation of an intermediate INTI, in which a new three-membered ring N(1)C(6)C(2) fused to the five-membered pyrrole ring is formed. The structure and the geometrical parameters of the transition state TS1 are closer to the parameters in the intermediate than to the parameters of *N*-methylene pyrrole, except for those of the methylene group (see Figure 2). The methylene group migration from N(1) to C(2) causes a deformation of the pyrrole ring, which can be seen in Table 1.

In *N*-methylene pyrrole, all the carbon atoms are in the sp^2 hybrid state, having bond lengths of 1.084 to 1.086 Å. In the intermediate INTl, the carbon atoms of the three-membered ring, C(2) and C(6) (Figure 2) are in the sp^3 hybrid state, having C−H bond lengths of 1.092, 1.091, and 1.090 Å for H(1)−C(2), H(5)−C(6), and H(6)−C(6), respectively. The C−H bonds of the pyrrole ring in the intermediate are also longer than the respective bonds in *N*-methylene pyrrole, indicating some loss of the definite sp^2 hybrid state. Both C−N bonds in the new ring have the same length, and the two rings have a dihedral angle of about 70°. The pyrrole ring in the intermediate loses its planarity to some extent (τ-N(1)C(2)C(3)C(4) is 3.37°) and its aromaticity. The bonds C(3)−C(4) and C(4)−C(5) have practically the same length, 1.397 and 1.394 Å, respectively, and the electron density is evenly distributed between C(3) and C(5), indicating the existence of a resonance structure in the intermediate.

The intermediate INTl forms orthohydropyridyl via transition state TS2. The main process in obtaining the transition state is a N(1)−C(2) bond rupture and expansion of the five-membered pyrrole ring to form the pyridine ring. The reaction coordinate is a N(1)−C(2) bond stretch combined with a N(1)C(6)C(2) angle bend (Figure 2). The bond distances C(4)−C(5) and N(1)−C(5) are practically the same and are between those of single and double bonds, pointing again to the existence of a resonance structure. In the final product hydropyridyl radical, the pyridine ring resumes the planarity that was lost in the formation of the intermediate INT1 from *N*-methylene pyrrole. The ring has two clear double bonds, C(2)−C(3) and N(1)−C(5). The C(6)−H(5) and C(6)−H(6) bonds are stretched to 1.109 Å as compared to 1.091 and 1.090 Å in the intermediate and 1.086 in *N*-methylene pyrrole. This stretching indicates weakening of these two bonds, which facilitate the ejection of one hydrogen atom and the formation of pyridine.

The ring expansion process of *N*-methylene pyrrole is rather simple, and low-energy barriers of the two transition states on the surface (Table 4) characterize it. In TS1 bonds are only formed and are not broken, and in TS2 breaking of the N(1)−C(2) bond (Figure 2) releases a large amount of the strain energy. This two-fused ring structure in INT1 is resonance-stabilized, a fact which expresses itself by the equal bond distances of C(3)−C(4) and C(4)−C(5).

2-Methylene Pyrrole. The ring expansion pathways of 2-methylene pyrrole are shown in Figure 3. The process of ring

TABLE 4: Total Energies E_{total} (in au), Zero-Point Energies,[a] Relative Energies ΔE,[b] and Entropies[c] for *N*-Methylene Pyrrole Ring Expansion, Calculated at uB3LYP/cc-pVDZ and uB3LYP/aug-cc-pVDZ Computational Levels

	uB3LYP/cc-pVDZ				uB3LYP/aug-cc-pVDZ			
species	E_{total}	ZPE	S	ΔE	E_{total}	ZPE	S	ΔE
N-methylene pyrrole	−248.837170	58.77	74.81	0.0	−248.853101	58.91	74.24	0.0
N-methylene pyrrole (MP2-fc[d])	−248.046649	62.51	77.57	0.0				
TS1	−248.779616	57.93	71.59	35.28	−248.795647	57.90	71.62	35.04
TS1 (MP2-fc[d])	−247.990604	59.04	74.22	38.58				
INT1	−248.800174	59.24	71.24	23.69	−248.816032	62.13	71.29	26.48
TS2	−248.780240	58.17	71.74	35.12	−248.797544	58.24	71.50	34.18
orthohydropyridyl	−248.843547	59.44	73.14	−3.32	−248.859967	59.41	73.31	−3.81

[a] Zero-point energies in kcal/mol ZPE were scaled by the ZPE scaling factor of 0.9806.[23] [b] Relative energies in kcal/mol $\Delta E = \Delta E_{total} + \Delta$(ZPE). [c] Entropies in cal/(K·mol). Entropies were scaled by the entropy scaling factor of 1.0015.[23] [d] ZPE and entropies calculated by uMP2-fc/cc-pVDZ were scaled by scaling factors of 0.967 and 1.044, respectively.[23]

TABLE 5: Total Energies E_{total} (in au), Zero-Point Energies,[a] Relative Energies ΔE,[b] and Entropies[c] for 2-Methylene Pyrrole Ring Expansion, Calculated at Different uB3LYP/cc-pVDZ and uB3LYP/aug-cc-pVDZ Computational Levels

	uB3LYP/cc-pVDZ				uB3LYP/aug-cc-pVDZ			
species	E_{total}	ZPE	S	ΔE	E_{total}	ZPE	S	ΔE
2-methylene pyrrole	−248.858900	59.28	73.71	0.0	−248.876237	59.34	73.58	0.00
TS3	−248.776653	56.91	75.50	49.20	−248.795143	56.93	75.57	48.49
INT2	−248.791936	57.09	80.91	39.83	−248.811535	57.20	81.14	38.46
TS4	−248.699900	54.19	79.86	94.58	−248.720905	54.35	79.87	92.49
TS5	−248.752471	57.46	74.32	64.95	−248.771223	57.46	74.45	64.03
INT3	−248.782989	59.52	74.56	47.88	−248.801464	59.54	74.89	47.13
TS6	−248.737524	56.55	73.50	73.38	−248.756233	56.57	73.50	72.53
N-hydropyridyl	−248.855207	59.80	73.68	2.84	−248.873330	59.56	75.79	2.05

[a] Zero-point energies in kcal/mol ZPE were scaled by the ZPE scaling factor of 0.9806.[23] [b] Relative energies in kcal/mol $\Delta E = \Delta E_{total} + \Delta$(ZPE). [c] Entropies in cal/(K·mol). Entropies were scaled by the entropy scaling factor of 1.0015.[23]

TABLE 6: Total Energies E_{total} (in au), Zero-Point Energies,[a] Relative Energies ΔE,[b] and Entropies[c] for 3-Methylene Pyrrole Ring Expansion, Calculated at Different uB3LYP/cc-pVDZ and uB3LYP/aug-cc-pVDZ Computational Levels

	uB3LYP/cc-pVDZ				uB3LYP/aug-cc-pVDZ			
species	E_{total}	ZPE	S	ΔE	E_{total}	ZPE	S	ΔE
3-methylene pyrrole	−248.851047	59.24	73.82	0.0	−248.868583	59.31	73.71	0.00
TS7	−248.731767	56.04	79.61	71.59	−248.750730	55.95	81.47	70.60
INT4	−248.732039	56.17	85.49	71.55	−248.751020	56.36	83.53	70.82
TS8	−248.620595	53.43	82.49	130.69	−248.640703	53.05	82.88	136.62
TS9	−248.745473	57.86	72.08	64.87	−248.764114	58.04	71.96	64.29
INT5	−248.751725	58.99	72.37	61.87	−248.769570	59.03	72.44	61.85
TSIO	−248.748493	58.78	71.45	63.89	−248.766691	58.84	71.44	63.47
INT6	−248.759779	59.67	73.11	57.70	−248.779348	59.81	73.15	56.50
TS11	−248.732276	56.58	73.24	71.87	−248.750934	56.61	73.22	71.13
N-hydropyridyl	−248.855207	59.80	73.68	−2.05	−248.873330	59.56	75.79	−1.70

[a] Zero-point energies in kcal/mol ZPE were scaled by the ZPE scaling factor of 0.9806.[23] [b] Relative energies in kcal/mol $\Delta E = \Delta E_{total} + \Delta$(ZPE). [c] Entropies in cal/(K·mol). Entropies were scaled by the entropy scaling factor of 1.0015.[23]

expansion begins with extension of the N(1)−C(2) bond. The initial bond length of 1.40 Å in 2-methylene pyrrole extends to 2.16 Å in TS3, which means that the bond is practically broken. The reaction coordinate is composed of two normal modes, N(1)−C(2) rupture and a rotation of the methylene group H(5)-C(6)H(6), with respect to the ring plane. The methylene group, in the transition state and in the intermediate INT2 that follows, appears as part of an allene structure, namely −C(3)H(2)═C(2)═C(6)H(5)H(6).

In the intermediate INT2, which is formed via transition state TS3 (Figure 3 and Table 2), the N(1)−C(2) distance is 3.02 Å. The planarity, which is lost in TS3, is regained in the intermediate INT2. The dihedral angles N(1)C(2)C(3)C(4) and N(1)C(6)C(3)C(4) of 9° and 16° in the transition state TS3 are zero in the intermediate.

It is interesting to point out the marked difference between the structure of the critical points of the *N*-methylene pyrrole ring expansion pathway (TS1 and INT1, Figure 2) and the equivalent points in the 2-methylene pyrrole pathway (TS3 and INT2). Whereas both TS1 and INT1 have a double-ring structure, namely five-membered and three-membered rings fused together, both TS3 and INT2 have an open structure. Formation of a double-ring structure in the pathway of 2-methylene pyrrole by the formation of a C(6)−N(1) bond would require a four valence nitrogen which cannot be obtained in neutral systems. On the other hand, the formation of a C(6)−C(3) bond in the transition state as the first step in the methylene group insertion into the pyrrole ring (between atoms C(2) and C(3)) could also lead to a double-ring structure. However, despite numerous attempts, a transition state of this nature could not be located.

The intermediate INT2 is transferred to hydropyridyl radical via two different routes. One route (#1) leads from INT2 to hydropyridyl directly via a high-energy transition state TS4 (Figure 3). The second route (#2) contains another intermediate INT3 with the involvement of two transition states, TS5 and TS6.

A. Route #1. The reaction coordinate in the transition state TS4 is a combination of two normal modes, H(5) atom shift from C(6) to C(2) and a C(6)C(2)C(3) angle bend. The H(5)−C(6) and H(5)−C(2) distances are 1.324 and 1.221 Å, respec-

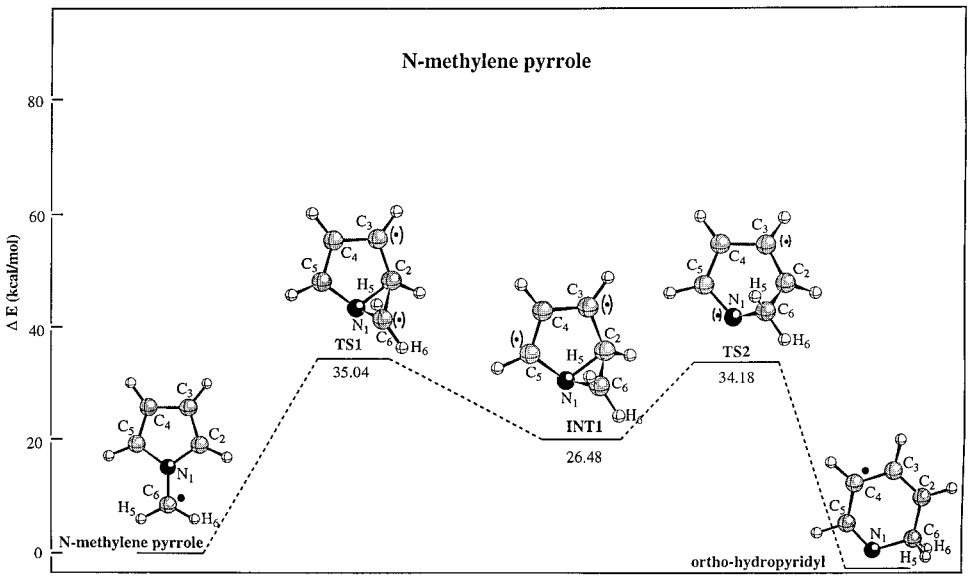

Figure 2. Potential energy profile of the ring expansion in *N*-methylene pyrrole. Relative energies Δ*E* (in kcal/mol) are calculated at uB3LYP/aug-cc-pVDZ level of theory. The energy levels include zero-point energies. The symbol (•) denotes high spin density.

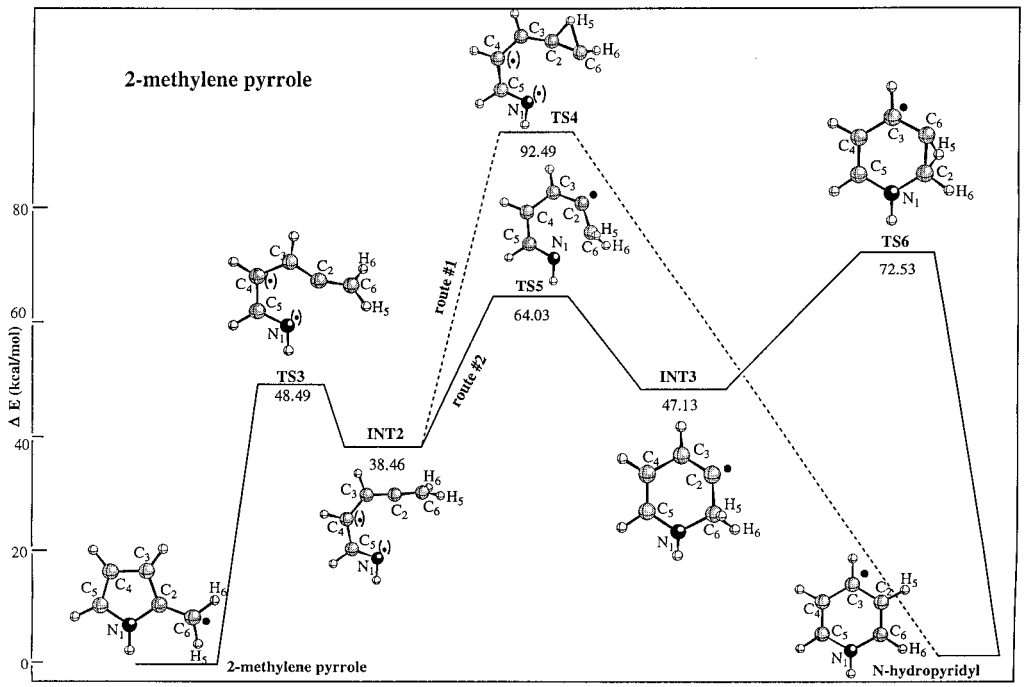

Figure 3. Potential energy profile of the ring expansion in 2-methylene pyrrole. Relative energies Δ*E* (in kcal/mol) are calculated at uB3LYP/aug-cc-pVDZ level of theory. The energy levels include zero-point energies. The symbol (•) denotes high spin density.

tively. The angle bend (Figure 3) is expressed also by the change of the dihedral angle H(6)C(6)C(2)C(3), which varies from 91° in the intermediate to 122° in the transition state.

B. Route #2. The transition state TS5 which connects the two intermediates INT2 and INT3 is still an open structure, but the linear string C(6)C(2)C(3) in INT2 has been drastically bended so that the distance C(6)−N(1) has been shortened from 3.636 Å in the intermediate to 1.989 Å in TS5 (Figure 3). Also, TS5 is no longer planar. The shortening of the distance facilitates the formation of a C(6)−N(1) bond, which can be seen in the intermediate INT3. What is still required to form a hydropyridyl radical is simply an H-atom shift from C(6) to C(2). This is the reaction coordinate in the transition state TS6. The carbon atom C(6) in the intermediate INT3, which is in the sp^3 hybrid state, is way out from the ring plane. In the transition state TS6 that connects INT3 to hydropyridyl, the reaction coordinate is a 1,2-H-atom shift from C(6) to C(2), where the C(6)−H(5) and C(2)−H(5) distances are 1.288 and 1.417 Å, respectively. In this transition state, the six-membered ring approaches the planarity typical to *N*-hydropyridyl.

Note that the hydropyridyl radical, which is obtained from 2-methylene pyrrole (orthohydropyridyl), is different from the one that is obtained from *N*-methylene pyrrole. Here the hydrogen atoms are evenly distributed on the six atoms of the pyridine ring. Removal of a hydrogen atom from the nitrogen produces pyridine. In order to produce pyridine from orthohydropyridyl radical, one hydrogen is removed from C(6). In both cases these are very fast processes.

From an energetic viewpoint, a marked difference between the ring expansion pathways of *N*-methylene pyrrole and 2-methylene pyrrole is the fact that the first stage in the latter is cleavage of the N(1)−C(2) bond, both in the transition state

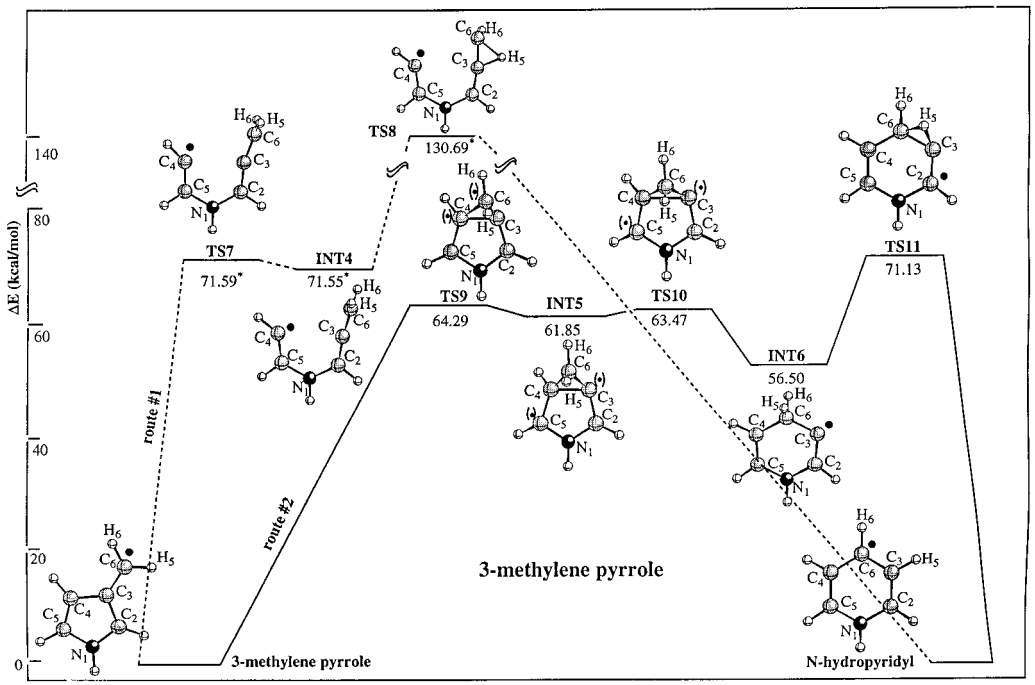

Figure 4. Potential energy profile of the ring expansion in 3-methylene pyrrole. Relative energies Δ*E* (in kcal/mol) are calculated at uB3LYP/aug-cc-pVDZ level of theory. The energy levels include zero-point energies. The symbol (•) denotes high spin density. The values marked with * were calculated at uB3LYP/cc-pVDZ level of theory.

TS3 and in the intermediate INT2 (Figure 3), whereas in *N*-methylene pyrrole the pyrrole ring stays intact (Figure 2). This clearly affects the energy levels of TS1 and TS3, the latter being at a higher level (Tables 4 and 5). As can be seen in Figure 3, the potential energy surface is more complicated than that of *N*-methylene pyrrole in the sense that the intermediate INT2 is connected to *N*-hydropyridyl via two different pathways. One route, which goes in one step from the intermediate INT2 to *N*-hydropyridyl, has a high barrier transition state, TS4, which lies about 92 kcal/mol above 2-methylene pyrrole. The second route is composed of two transition states, TS5 and TS6, and an intermediate, INT3. The highest energy level in this route is that of TS6 and it lies about 73 kcal/mol above 2-methylene pyrrole. Although the first route is more direct, the high energy level of TS4 prevents this route from contributing to the process.

3-Methylene Pyrrole. The pathway for the production of *N*-hydropyridyl from 3-methylene pyrrole is shown in Figure 4. As can be seen, there are two different routes that lead to ring expansion of 3-methylene pyrrole to *N*-hydropyridyl. One channel (route #1) is similar to the ring expansion channel of 2-methylene pyrrole. The pyrrole ring breaks and an open structure intermediate is formed. The second channel (route #2) resembles the behavior of *N*-methylene pyrrole, namely, no formation of an open structure toward the production of *N*-hydropyridyl. There is a difference between the ring expansion process of 3-methylene pyrrole and that of the other two isomers. Whereas the transition states and intermediates in the latter involve cleavage of the C−N bond somewhere along the pathway, in 3-methylene pyrrole ring expansion, the C-N bond stays intact and the C(3)−C(4) bond is broken.

A. Route #1. As has been mentioned before, this pathway is similar to that of 2-methylene pyrrole → *N*-hydropyridyl. This can be seen in Figures 3 and 4. In both cases there are two transition states and one intermediate along the reaction channel. They are marked on the 3-methylene pyrrole potential surface as TS7, TS8, and INT4. The first stage (TS7) involves the opening of the pyrrole ring by cleavage of the C(3)−C(4) bond, and the second stage (TS8) is a 1,2-H-atom shift together with a shortening of C(6)−C(4) distance, which facilitates the formation of a six-membered ring. The reaction coordinate is C(3)−C(4) bond stretch together with C(2)N(1)C(5) angle increase and a rotation of the methylene group H(5)C(6)H(6) with respect to ring plane, as has been observed in the equivalent transition state of the first stage in 2-methylene pyrrole (TS3 in Figure 3). The angle C(2)N(1)C(5) increases from 110° in 3-methylene pyrrole to 120° in the transition state TS7 and 124° in the intermediate INT4 (Table 3). The C(3)−C(4) distance changes from 1.451 Å in 3-methylene pyrrole to 2.559 Å in the transition state, and further to 2.807 Å in the intermediate. Also, the formation of an allene structure −C(2)H(2)═C(3)═C(6)H(5)H(6), both in the transition state TS7 and the intermediate INT4, can be seen.

The reaction coordinate in the second stage of 3-methylene pyrrole isomerization, namely INT4 → TS8 → *N*-hydropyridyl, is a 1,2-H-atom shift from C(6) to C(3). The C(4)−C(6) distance in the transition state is still large, but it is somewhat shorter than the distance in INT4. It is interesting to note that in all the intermediate structures along the 3-methylene pyrrole ring expansion pathway, i.e., the two transition states TS7 and TS8 and the intermediate INT4 (Figure 4), the electron density is fully localized on C(4) with a spin density around unity. Along the ring expansion pathway in route #1 of 2-methylpyrrole, however, which is very similar to the pathway of 3-methylene pyrrole just discussed, the electron density is distributed between one carbon atom, C(4), and the nitrogen atom, N(1).

B. Route #2. Whereas route #1 is similar to the first stage of the ring expansion pathway in 2-methylene pyrrole in the sense that the pyrrole ring is already open in the first transition state, route #2 is similar to the route in *N*-methylene pyrrole, where the pyrrole ring stays intact. However, route #2 in 3-methylene pyrrole has an additional intermediate and transition state. Altogether there are three transition states, TS9, TS10, and TS11, and two intermediates, INT5 and INT6 (Figure 4). The reaction coordinate of the first stage (TS9) is a decrease of the C(6)-

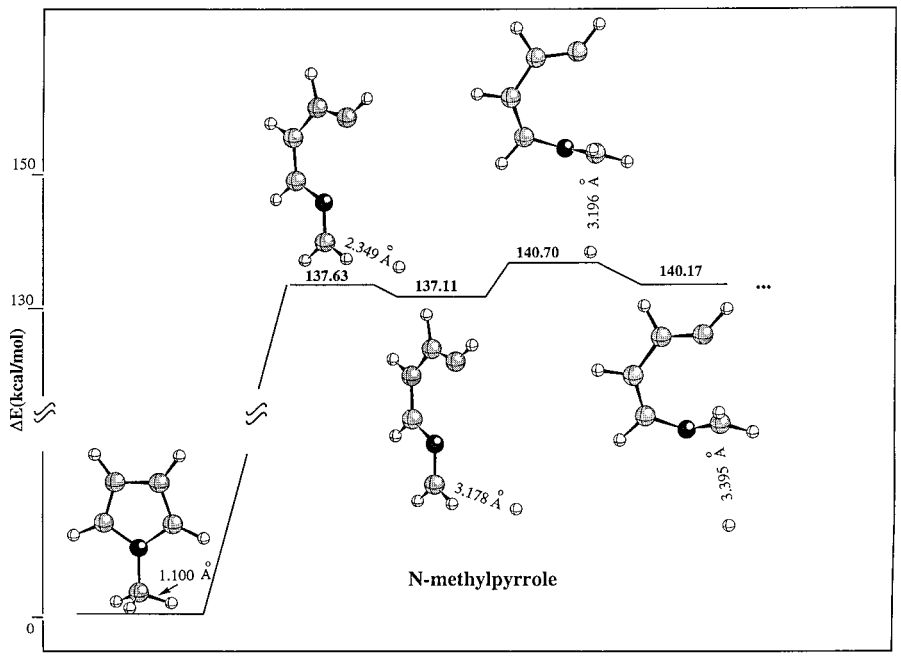

Figure 5. Potential energy profile of *N*-methylpyrrole ring expansion. Relative energies ΔE (in kcal/mol) are calculated at B3LYP/cc-pVDZ level of theory. The energy levels include zero-point energies. The reaction coordinate is both cleavage of the C−N bond and ejection of a H-atom from the methyl group.

C(3)C(4) angle together with a rotation of the methylene group C(6)H(5)H(6) with respect to the pyrrole ring plane. This results in shortening C(4)−C(6) distance from 2.564 Å to 1.789 A, toward the formation a new three-membered ring C(3)C(4)-C(6) similar to TS1 (Figure 2). The intermediate INT5 already has two fused rings, a new three-membered ring and the original pyrrole ring. The spin density in the intermediate is almost evenly distributed on atoms C(3) and C(5). In both TS9 and INT5, the pyrrole ring loses its planarity, somewhat similarly to what has been observed in TS1 and INT1. Also, the dihedral angle between the two rings is practically the same, about 68°.

In the second stage of this route, the two fused rings in INT5 turn into a six-membered pyridine ring via transition state TS10. This stage is very similar to the *N*-methylene pyrrole route, except that in *N*-methylene pyrrole the final product is the orthohydropyridyl radical, and here it is an intermediate which still requires a 1,2-atom migration from C(6) to C(3) in order to form a hydropyridyl radical.

Transition state TS10 (Figure 4) is not only very similar to transition state TS2 (Figure 2); it also has the same reaction coordinate: C(3)−C(4) bond stretch combined with C(3)C(6)-C(4) angle bend. The difference between TS2 and TS10 is the absence of resonance in TS10. (TS9 and INT5 also have no resonance structure.) The intermediate INT6 turns to the product *N*-hydropyridyl via the transition state TS11 (Figure 4). The last process is 1,2-H-atom shift from C(6) to C(3).

Whereas both intermediates and transition states in all the pathways of *N*-methylene pyrrole and 2-methylene pyrrole have either closed (*N*-methylene pyrrole) or open structures (2-methylene pyrrole), 3-methylene pyrrole has both open and closed structures in its ring expansion pathways. The open structure pathway, which is characterized by transition states TS7 and TS8, is the high-energy pathway with the highest barrier of approximately 136 kcal/mol (Table 6). The second, closed structure pathway contains two intermediates and three transition states, the highest of which lies about 71 kcal/mol above 3-methylene pyrrole.

V. Ring Expansion in the Molecule *N*-Methylpyrrole

We tried to find a reaction pathway for the ring expansion of the molecule *N*-methylpyrrole. Although the pathway is not complete, its characteristics are very clear. The potential energy surface of this pathway is shown in Figure 5. The first stage is rupture of the N−C bond together with H-atom ejection from the methyl group. The pathway includes several transition states and intermediates in which the C−H distance increases in each step. The final product is practically a pair of radicals that are a hydrogen atom and orthohydropyridyl. The very high-energy barriers of about 140 kcal/mol are the result of C−H and C−N bond cleavage. From a kinetic viewpoint this pathway is almost equivalent to two steps, H-atom ejection and ring expansion:

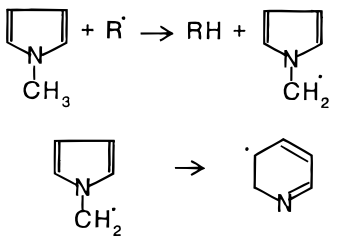

VI. Dependence of Geometry and Energetics on Choice of Basis Set

The difference in the values of the structural parameters obtained by the two basis sets aug-cc-pVDZ and cc-pVDZ does not exceed 0.04 Å for bonds that are not involved in the reaction coordinate. For long distances between atoms resulting from bond breaking either along the reaction coordinate or toward the formation of new bond, the difference between the two basis sets sometimes reached values of up to 0.3 Å. The difference in the angles between bonds does not exceed 1°. The effect of the basis set on the dihedral angles was more significant particularly when bonds with both heavy atoms and hydrogen formed the angles. The differences in some cases were close to 10°, but were around 1° for cases where only heavy atoms were

considered. We found also that when the reaction coordinate indicated loss of planarity of the rings (distortion of C_s symmetry), the loss was less significant with the augmented basis set. In all cases, C−H bonds with the aug-cc-pVDZ basis set were shorter.

The energetics of the species involved in the isomerization of methylene pyrrole are shown in Tables 4−6 for both the cc-pVDZ and the aug-cc-pVDZ basis sets. In all the cases, the aug-cc-pVDZ basis set gave lower values for the energy barriers, the difference being up to 2 kcal/mol. The exception is 3 kcal/mol for INTl.

We have also run, for comparison, the structure and energetics of *N*-methylene pyrrole and the transition state TS1 using ab initio frozen-core MP2/cc-pVDZ. The results of this calculation are shown in Table 4. For TS1, the agreement between DFT and MP2 calculations is quite good. For *N*-methylene pyrrole, the optimized structure and the frequencies using MP2 came out a little different than the structure and the frequencies obtained by DFT. This caused a difference in the zero-point energy, and thus the level of the transition state came out 3.3 kcal/mol higher.

VII. Chemical Kinetic Considerations

Rate Parameters. The Arrhenius first-order rate constants for the three-ring expansion processes were calculated from the relation:[25]

$$k_{\infty} = \sigma(ekT/h)\exp(\Delta S^{\#}/R)\exp(-E_a/RT) \qquad (1)$$

where ΔS and E_a correspond to the difference between the transition state of the highest barrier and the correspondent reactant. The values obtained are:

$$k_{N-\text{methylene pyrrrole}} = 10^{13.04}\exp(-35.0\times10^3/RT)\ \text{s}^{-1} \qquad (2)$$

$$k_{2-\text{methylene pyrrrole}} = 10^{13.30}\exp(-72.5\times10^3/RT)\ \text{s}^{-1} \qquad (3)$$

$$k_{3-\text{methylene pyrrrole}} = 10^{13.20}\exp(-71.1\times10^3/RT)\ \text{s}^{-1} \qquad (4)$$

Chemical Kinetic Aspects of Complicated Routes of Ring Expansion. We have performed a detailed kinetic analysis of the ring expansion pathway of *N*-methylene pyrrole, taking into account all the steps of route #2, which contains two intermediates. We have calculated first-order rate constants for each one of the steps and performed computer modeling to obtain profiles of [*N*-hydropyridyl]$_t$/[*N*-hydropyridyl]$_{eq}$ as a function of time. We then calculated first-order rate constant as if the reaction path were simply 2-methylene pyrrole → TS6 → *N*-hydropyridyl and obtained the same profiles. We used the relation:

$$(k_1 + k_{-1})t = -\ln\left(1 - \frac{[N\text{-hydropyridyl}]_t}{[N\text{-hydropyridyl}]_{eq}}\right) \qquad (5)$$

where k_l is the rate constant for the reaction 2-methylene pyrrole → *N*-hydropyridyl. A comparison between the two is shown in Figure 6, where [*N*-hydropyridyl]$_t$/[*N*-hydropyridyl]$_{eq}$ is plotted as a function of time. The filled circles in the figure represent the profile obtained from the modeling, and the solid line is calculated from the one-step reaction path. As can be seen, they are practically identical. We have artificially lowered the potential well of INT2 by 20 kcal/mol and again performed the computer modeling. The results are shown in Figure 6 as the open squares. As can be seen, there is only a small difference between these results and those obtained with the original potential well. The reason for the difference, however, is the accumulation of INT2. When the well is further lowered, the extent of the reaction decreases and concentration of INT2 increases.

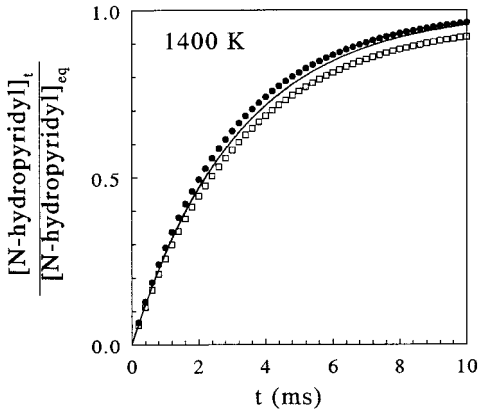

Figure 6. Plot of [*N*-hydropyridyl]$_t$/[*N*-hydropyridyl]$_{eq}$ as a function of time at 1400 K. The filled circles in the figure represent the profiles obtained from the modeling and the solid line calculated from the one-step reaction path (see text). The open squares are the best fit through points calculated by artificially lowering the potential well of the INT2 by 20 kcal/mol.

Comparison with Experimental Results. In a previous study on the decomposition of *N*-methylpyrrole,[3] we assumed that the production of pyridine took place via the ring expansion of *N*-methylene pyrrole (as has now been shown to be a correct assumption) and estimated a rate constant of $10^{14.0}\exp(-55.0\times10^3/RT)$ s^{-1} for this process, which is considerably smaller then the one obtained in the present calculations. Nevertheless, the agreement of the calculated rate of pyridine production with the experimental rate was agreeable. The reason is that the production rate of pyridine is much more sensitive to variations in the production rate of *N*-methylene pyrrole (both by ejection and abstraction of H-atoms from the methyl group of *N*-methylpyrrole) than to variations in the rate of the ring expansion process. In other words, the rate-determining step for pyridine production is not the ring expansion process. Also, the production of pyridine depends on the rates of other reactions in the kinetic scheme. The conclusion is that it is hard to provide a solid experimental support to the calculated value of the rate constant for ring expansion from the study of the decomposition of *N*-methylpyrrole.

VIII. Conclusions

The quantum chemical calculations presented in this article support the assumption regarding the radical character of the ring expansion reaction of five-membered pyrrole rings to six-membered pyridine rings. The ring expansion takes place from methylene pyrrole radicals by insertion of a methylene group into the five-membered pyrrole ring. The process of the methylene group insertion can occur via two principal mechanisms. One mechanism is associated with cleavage of the C−N or one of the C−C bonds in the pyrrole ring in the first stage. This mechanism can be seen in the routes where TS3 and TS7 are the transition states of the first stage. In the second mechanism, the transition states of the first stage are composed of a three-membered and the original pyrrole ring fused together (TS1 and TS9). In this mechanism the formation of the pyridine ring occurs when the three-membered ring is ruptured by breaking the bond which fused the two rings together. These two mechanisms have different energy characteristics.

The ring expansion from *N*-methylene pyrrole is much faster than the expansion from the other two isomers, 2- and 3-methylene pyrrole, because of the higher energy barrier of the latter. Because the three isomers interisomerize quite rapidly,[20] it is possible that ring expansion from 2- and 3-methylene pyrrole takes place from *N*-methylene pyrrole following the isomerization process.

Acknowledgment. This research was supported by Grant 9800076 from the United States−Israel Binational Science Foundation (BSF), Jerusalem, Israel. The authors thank also the Ministry of Absorption for a fellowship to F.D. in the frame of the Giladi program.

References and Notes

(1) Frank, P.; Herzler, J. T.; Wahl, C. In *Twenty-fifth Symposium (International) on Combustion*; The Combustion Institute: Pittsburgh, PA, 1994; p 833, and references cited therein.

(2) Tan, Y.; Frank, P. In *Twenty-sixth Symposium (International) on Combustion*; The Combustion Institute: Pittsburgh, PA, 1996; p 677.

(3) Lifshitz, A.; Shweky, I.; Tamburu, C. *J. Phys. Chem.* **1993**, *97*, 4442.

(4) Wiberg, K. B.; Cheeseman, J. R.; Ochterski, J. W.; Frish, M. J. *J. Am. Chem. Soc.* **1995**, *117*, 6535.

(5) Lui, R.; Francisco, J. S. *J. Phys. Chem.* **1998**, *102*, 9869.

(6) Mayer, P. M.; Parkinson, C. J.; Smith, D. M.; Radom, L. *J. Chem. Phys.* **1998**, *108*, 604.

(7) Vereecken, L.; Pierloot, K.; Peeters, J. *J. Chem. Phys.* **1998**, *108*, 1068.

(8) Rice, B. M.; Pai, S. V.; Chabalowski, C. F. *J. Phys. Chem.* **1998**, *102*, 6950.

(9) El-Azhary, A. A.; Suter, H. U. *J. Phys. Chem.* **1996**, *100*, 15056.

(10) Jursic, B. S. *J. Chem. Phys.* **1996**, *104*, 4151.

(11) Jursic, B. S. *J. Phys. Chem.* **1998**, *102*, 9255.

(12) Jursic, B. S. *J. Phys. Chem.* **1997**, *101*, 2345.

(13) Jursic, B. S. *Chem. Phys. Lett.* **1997**, *264*, 113.

(14) Jursic, B. S. *J. Mol. Struct.* **1996**, *365*, 75.

(15) Jursic, B. S. *Chem. Phys. Lett.* **1996**, *256*, 603.

(16) Becke, A. D. J. *Chem. Phys.* **1993**, *98*, 5648.

(17) Lee, C.; Yang, W.; Parr, R. G. *Phys. Rev.* **1988**, *B37*, 785.

(18) Dunning, T. H., Jr. *J. Chem. Phys.* **1989**, *90*, 107.

(19) Kendall, R. A.; Dunning, T. H., Jr.; Harrison, R. J. *J. Chem. Phys.* **1992**, *96*, 6796.

(20) Doughty, A.; Mackie, J. C.; Bacskay, G. B. *Chem. Phys. Lett.* **1994**, *221*, 267.

(21) Schlegel, H. B. *J. Comput. Chem.* **1982**, *3*, 214.

(22) Peng, C.; Schlegel, H. B. *Isr. J. Chem.* **1993**, *33*, 449.

(23) Scott, A. P.; Radom, L. *J. Chem. Phys.* **1996**, *100*, 16502.

(24) Frisch, M. J.; Trucks, G. W.; Schlegel, H. B.; Gill, P. M. W.; Johnson, B. G.; Robb, M. A.; Cheeseman, J. R.; Keith, T.; Petersson, G. A.; Montgomery, J. A.; Raha-vachari, K.; Al-Laham, M. A.; Zakrzewski, V. G.; Orviz, J. V.; Foresman, J. B.; Cioslowski, J.; Stefanov, B. B.; Nanayakkara, A.; Challacombe, M.; Peng, C. Y.; Ayala, P. Y.; Chen, W.; Wong, M. W.; Andres, J. L.; Replogle, E. S.; Gomperts, R.; Martin, R. L.; Fox, D. J.; Binkley, J. S.; Defrees, D. J.; Baker, J.; Stewart, J. P.; Head-Gordon, M.; Gonzalez, C.; Pople, J. A. *GAUSSIAN94*, revision D.4; Gaussian, Inc.: Pittsburgh, PA, 1995.

(25) Dubnikova, F.; Lifshitz, A. *J. Chem. Phys.* **1998**, *102*, 5876.